Two-Dimensional Displacement Sensor Based on Plastic Optical Fibers

Two-Dimensional Displacement Sensor Based on Plastic Optical Fibers

A. Vallan, M.L. Casalicchio, M. Oliviero, G. Perrone

Published in: Instrumentation and Measurement, IEEE Transactions on (Volume:62 , Issue: 5)
Date of Publication: May 2013
Page(s): 1233 - 1240
ISSN : 0018-9456
INSPEC Accession Number: 13412885
Digital Object Identifier : 10.1109/TIM.2012.2236725
Sponsored by : IEEE Instrumentation and Measurement Society

Two-Dimensional Displacement Sensor Based on Plastic Optical Fibers

Alberto Vallan, *Member, IEEE*, M. L. Casalicchio, M. Olivero, G. Perrone *Member, IEEE*

***Abstract*—An inexpensive fiber-based displacement sensor for two-dimensional crack monitoring is proposed and analyzed. The device is packaged as conventional crack monitoring gages based on sliding plates and exploits the dependence of the transmitted power between facing optical fibers with the displacement. The use of multi-core polymeric fibers with high numerical aperture allows a compact form factor and simplifies the sensor assembly. The position detection algorithm has been optimized through simulations; then experimental tests have shown a good agreement with simulations and have proved that even with simplified layout and artisanal realization the sensor can measure displacements in a square area of 3 mm by 3 mm with an uncertainty better than $50\ \mu\mathrm{m}$.**

I. Introduction

Structural Health Monitoring (SHM) is commonly associated with civil engineering applications, in which it is necessary to track the evolution of cracks in walls; but SHM is gaining a much broader relevance and it is becoming a paradigm, not only in the design of new civil structures and in cultural heritage preservation, but even in industrial applications.

Moreover, modern SHM is often associated with the concept of Condition-Based Maintenance (CBM), which stands for a set of tools and procedures devised to reduce the complexity and the cost in permanent diagnostics of small and large artifacts, from mechanical machines to large buildings. The present scenario foresees a massive exploitation of real-time monitoring SHM/CBM tools to improve safety and reliability, and reduce severe maintenance operations [1], [2].

Most of SHM and CBM applications require measuring displacements between two well-identified points, like in the case of crack monitoring, although using sensors having specific maximum operating range and resolution, depending on the considered materials. For example, cracks in masonry, marble or composite materials, all require sensors with different characteristics. If we restrict the survey to the diagnostic of cracks in concrete and masonry, the typical requirement for long-term evaluations is to measure a maximum displacement of about ± 1 cm, with a resolution in the order of 0.5 mm.

This can be achieved with mechanical extensometers, very cheap devices made by two plastic plates that can slide one on the top of the other, and having a reference crosshair engraved on one plate and a grid on the other [3]. These sensors are not compatible with remote interrogation requirements but, on the other hand, they are two-dimensional displacement sensors since they allow measuring the displacement on a plane.

More accurate - though typically one-dimensional - sensors include capacitive/resistive/inductive gauges [4] and optical fiber sensors [5].

However, situations exist where displacement measurements with higher resolution (e.g. at least 0.1 mm) although in a smaller range (usually few millimeters) are required. Examples include industrial applications, like the evaluation of the fatigue of machine parts, and the monitoring of artworks under restorations (e.g. ancient statues, vases, etc.), where the effects of on-off conditions or of day-night temperature variations must be precisely measured. In such cases, optical fiber sensors are generally preferred for their highest performance.

Glass optical fibers similar to those used in high performance communication links have emerged as an increasingly important technology tool for SHM/CBM due to their unique advantages in terms of sensitivity, multiplexing capability, low weight, little invasiveness, remote interrogation, as well as immunity to electromagnetic interference and impossibility to start fires. An extensive review of optical fiber sensors, including intensity-based, fiber Bragg gratings (FBG), Fabry-Perot and more, has been covered by a number of scientific publications [6], [7] and white papers [8]. On the other hand, in the last decade there has been also a rising interest in optical fiber sensors relying on Plastic Optical Fibers (POF). These fibers are typically made of a core in Poly-Methil-Meth-Acrylate (PMMA) surrounded by a cladding in fluorinated polymers. Most common POF have a core ranging from 250 μm to 980 μm, very thin cladding, and a numerical aperture of about 0.5, resulting in millions of guided modes. POF are usually operated in the visible spectral region, where they exhibit low loss, although much higher than that measured in glass fibers. Their main advantages over conventional glass fibers have been pinpointed as the ease of making connections and the simplified handling. Moreover, POF are particularly well suited for the fabrication of low cost sensors for the measurement of physical quantities and the detection of chemicals exploiting the variation of the received intensity through fiber spans [9], [10].

A number of POF intensity sensors have been proposed to measure displacements and vibrations [11], but these devices are intrinsically 1D-sensors since they detect displacements in one direction only. In many cases this is not a limitation because the displacement occurs predominantly along one direction, such as in the case of cracks in concrete beams. However, in other situations it is practically impossible to predict the direction of the displacement, which might even

M.L. Casalicchio, M. Olivero, G. Perrone and A. Vallan are with the Dipartimento di Elettronica e Telecomunicazioni, Politecnico di Torino, corso Duca degli Abruzzi, 24 - 10129 Torino (Italy); phone: +39 011 5644110, fax: +39 011 5644217, e–mail: alberto.vallan@polito.it This work has been supported by Piemonte local government within LASERFACTORY project: *"Next generation of machines based on fiber lasers for massive production in the automotive and aerospace industry"* (Bando Sistemi di produzione 2008).

change randomly over time.
For these reasons, it would be more convenient to have a compact true 2D-fiber sensor and this paper addresses the problem by describing a low-cost POF sensor able to measure small displacements on a plane. The paper is organized as follows: in Sect. II the sensor working principle is discussed, in Sect. **??** the impact on the performances of the sensor realization parameters is analyzed, then in Sect. **??** experimental results from a sensor prototype are presented. Finally in Sect. V the conclusion are drawn.

II. Sensor working principle

The developed 2D-POF sensor resembles a typical commercial mechanical crack monitoring device [3].
Two plastic plates, designed to be fixed at the sidewalls of the region whose displacement has to be monitored (crack in the following for simplicity), are superimposed and can slide in two dimensions according to the crack evolution, like in Fig. 1(a). One of the plates embeds a transmitting fiber and the other plate some receiving fibers arranged in a bundle to form a displacement sensor that exploits the variation of received power between facing fibers with lateral misalignment, as shown in Fig. 1(b) and in Fig. 1(c). Although the cases of three and four receiving fibers have been studied in detail, in the following, the reported results are for the case of three receiving fibers only because this represents the minimal configuration suitable to implement the proposed 2D displacement sensor.
In order to reduce the form factor, both transmitting and receiving fibers are embedded into the plates horizontally; then to deflect the light by 90° the reflection from a miniaturized prism or a metal-coated metered angular cleave can be exploited.
Alternatively, if the plate thickness is not a primary concern, the signal deflection problem can be simplified using multicore plastic optical fibers, since they accept much narrower curvature radii without significant increase in the propagation loss. Using multicore fibers has the further advantage of lowering the sensitivity to external environmental disturbances of the fiber span between the sensor and the interrogation unit, a property particularly interesting in long-term monitoring applications.

The upper and lower parts of the sensor are aligned so that, with a null displacement, the axis of the transmitting fiber is facing the center of mass of the receiving fiber constellation, as shown in Fig. 2 for the cases of three and four receiving fibers. This way, a null displacement corresponds to equal power at the receivers. The amount, direction and versus of the displacement in the (x-y) plane between the two plates are evaluated from the variations of the power at the receivers, in a way similar to that used in conventional intensity-based displacement sensors.

Prior to running the experiments, simulations have been carried out to evaluate the sensor performances in ideal conditions.

The received power from each fiber is a function of the relative position with respect to the transmitting fiber and,

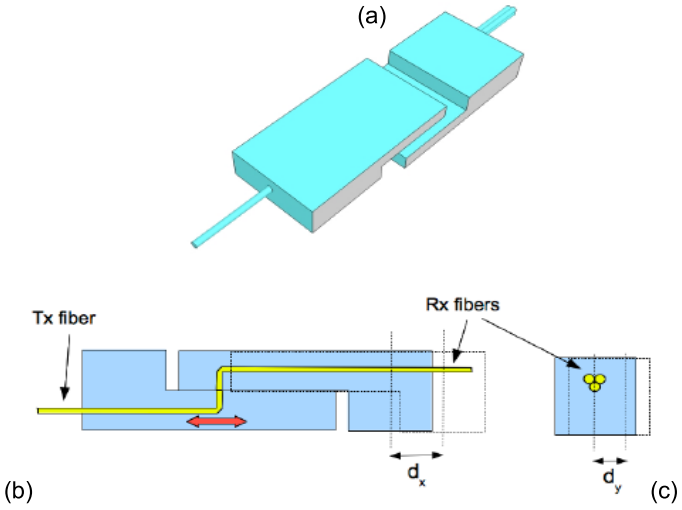

Fig. 1. A drawing schematic representation of the sensor prototype (a); lateral (b) and front views (c).

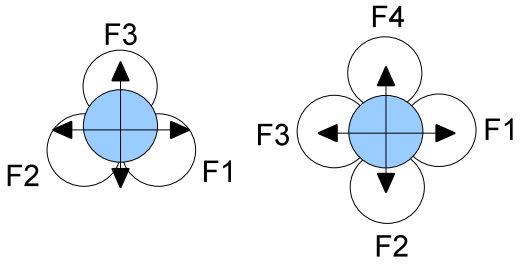

Fig. 2. Schematic representation of the ideal zero displacement position of transmitting (blue circle) and receiving (clear circles) fibers for the cases of three (left) and four (right) receivers, respectively.

given the highly multimode working condition, it can be computed using well-known models based on geometrical considerations [12].

The light intensity distribution, I in Fig. 3, can be approximated with a Gaussian shape [13] having the most significative part of the optical power (typically 95%) confined inside an

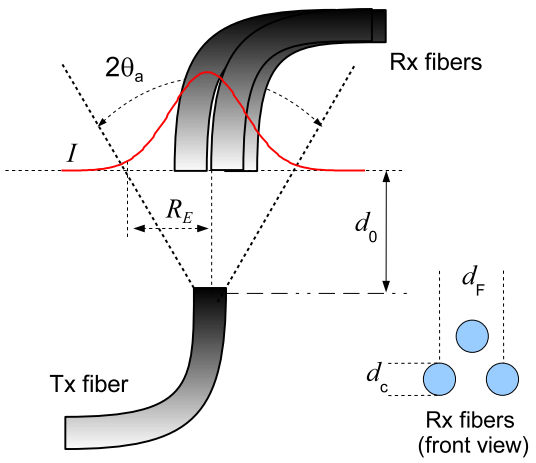

Fig. 3. Sensor structure (three receiving fiber case) and light intensity distribution at the receiving fiber tips.

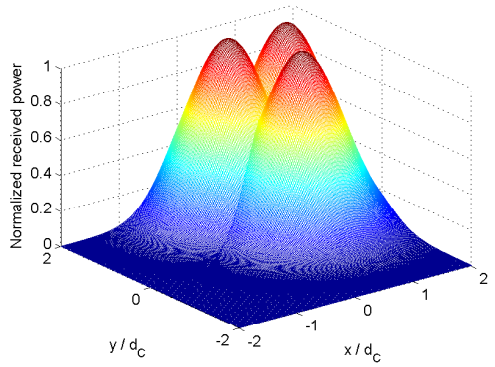

Fig. 4. Optical power collected by the receiving fibers as a function of the transmitting fiber position (x,y) normalized to the fiber diameter d_c.

emitting cone whose aperture angle $2\theta_a$ is related to fiber numerical aperture (NA) as:

$$\theta_a = \arcsin(\mathrm{NA}) \tag{1}$$

The illuminated area at the receiving fiber position can be thus approximated as a circle, whose radius R_E is related to the distance d_0 between the fiber tips, to the diameter of the fiber core d_c and to the numerical aperture as:

$$R_E = \frac{d_C}{2} + d_0 \cdot \tan(\theta_a) \tag{2}$$

When the receiving fiber is located inside the illuminated circle it collects a significant amount of optical power that can be computed integrating the light intensity over the receiving fiber surface [13]. As an approximation, the received power can be considered uniform over the receiving fiber tip, thus resulting in a Gaussian distribution of the received optical power. Nevertheless, an analytical model describing the light intensity at the POF output can just approximate the actual intensity since, due to the highly multimodal working conditions, these fibers are strongly sensitive to the characteristics of the source (wavelength, spatial distribution, alignment, etc. even for long fiber spans) and to the strains along the fiber, so in practice it is difficult to be in modal equilibrium for all the working conditions. For these reasons, some authors investigated different light distribution models [14] whose parameters have to be obtained by fitting experimental data when a high accuracy is required. Anyway, experimental tests previously carried out by the authors both using single- and multi-core fibers, have shown that in the case of interest the received power behavior can be still approximated with a Gaussian function regardless the actual intensity distribution due to the spatial averaging operated by the large surface of the receiving fibers.

An example of the received power versus transmitting fiber position for the three receiving fiber case is reported in Fig. 4. In the figure the power is normalized to have unit value when the transmitting and the corresponding receiving fibers are perfectly overlapped. Moreover, since all the fibers of the receiving bundle have the same diameter, they exhibit similar output levels but with the peak intensity located in a different position of the plane.

Similar curves are obtained for the four or more receiving fiber cases. It should be noted that the proposed sensor configuration is not that of typical 2D-fiber arrays, although it has some similarities, especially in the case of four or more receivers. Indeed, plates with a large number of equispaced fibers distributed in a squared area are commercially available (see for example [15]), but, using glass fibers, these setups cannot be employed to meet the specifications for the application target in this paper. In particular, the use of standard telecom-grade glass fibers implies to have small cores with relatively large core-to-core distance and low numerical aperture, with a substantial reduction in the working range, besides for the costs associated with sources, connectors and receivers suitable for glass fibers. On the contrary, given their large core-to-cladding diameter ratio and large numerical aperture, the use of standard step index polymeric fibers positioned as proposed in this paper yields to a good compromise between working range and resolution. Moreover, POF allow also a dramatic decrease in the overall system cost, which becomes comparable with that of electro-mechanical devices.

III. Measurement of the Transmitting Fiber Position

As already mentioned, displacements in the (x,y) plane are then evaluated by analyzing the readings of the receiving fibers. With specific reference to the three receiver case, Fig. 5 shows two examples of diagonal and horizontal displacements with respect to the ideal zero position in which the amount of the received power is the same from each fiber.

It is clear from Fig. 5 that by comparing the readings of the three received light intensities, it is possible to identify the direction and versus of the movement and to measure the amount of displacement.
In principle, a 2-D movement should require just two readings to be identified, but in practice at least three fibers are necessary to avoid versus ambiguity due to the symmetry in the fiber response with lateral misalignments.

A simple position detection algorithm has been developed to recover the relative position of the two plates from the received optical power. Given the fiber symmetry, the region on the plane corresponding to a constant power value collected by a receiving fiber (equi-power curve) is a circumference centered on the considered receiving fiber and with radius increasing as the power value decreases. Consequently, the position of the transmitting fiber can be found as the intersection of three circumferences representing the respective received power levels. For this, at least three receiving fibers are necessary, as shown in Fig. 6.

The sensor maximum range can be estimated considering that all the receiving fibers must collect a certain amount of the transmitted light so the receiving fiber tips must be located inside the light cone produced by the transmitting fiber. Fig. 7 shows the light spot and the receiving fiber tips when the transmitting fiber is located at the far left (light spot #1) and far right (light spot #2) positions. The sensor range SR can

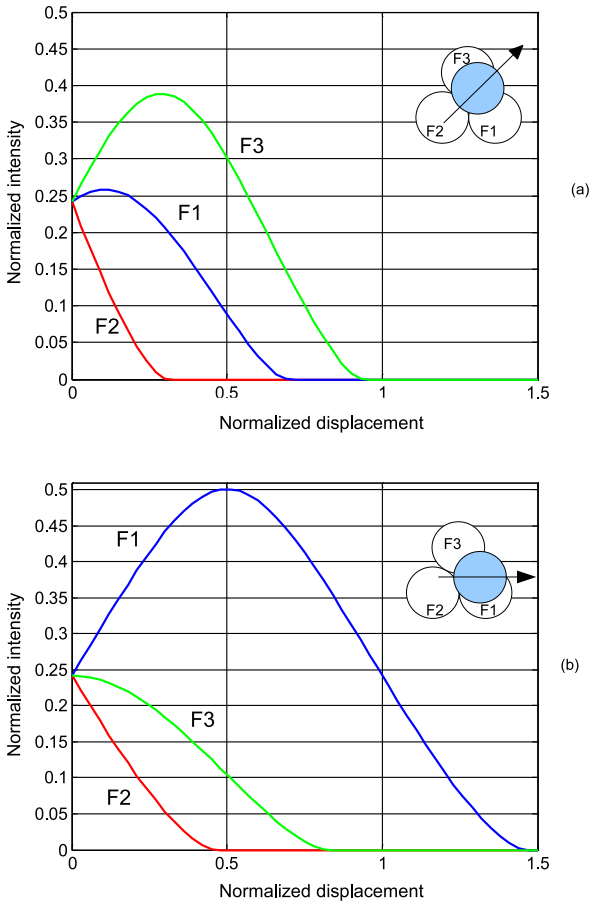

Fig. 5. Simulation of the expected readings for a diagonal (a) and horizontal (b) displacement of the transmitting fiber. The displacements have been normalized with respect to the radius of the fibers, while the intensity is normalized to have unitary value when the transmitting fiber is exactly facing a receiving fiber.

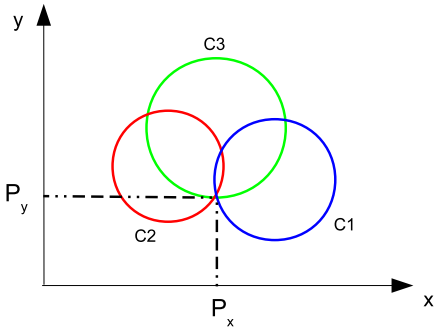

Fig. 6. Position detection algorithm: the relative position of the two plates is evaluated considering the intersection of the three constant power circumferences representing the received signal intensity from the receiving fibers.

be therefore obtained as the distance of these two extreme positions, and can be approximated as:

$$\mathrm{SR} \simeq 2\,R_{\mathrm{E}} - d_{\mathrm{F}} + d_{\mathrm{c}} \tag{3}$$

The quantity SR depends on fiber diameter and spacing, as well as on the emitting cone radius R_{E} that, in turn, depends

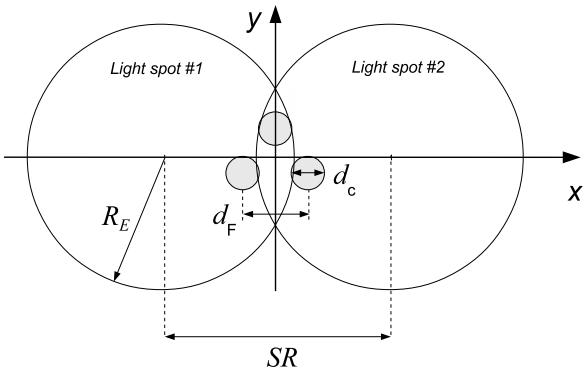

Fig. 7. The area illuminated by the transmitting fiber when positioned at the two opposite ends of the sensor working range.

on the distance d_0 between the transmitting and receiving fiber tips. Larger distances lead to wider sensor ranges but also to a reduction in the collected power and thus to larger uncertainties. Therefore, the distance d_0 must be chosen as a trade-off between range and performance. In the case of four receiving fibers, the operating range is extended because, with the addition of an extra fiber, the position is recovered from the intersection of the three circumferences out of four having the highest received power.

A better evaluation of the expected sensor operating range can be derived by taking into account the gaussian optical power distribution and considering the light detector noise as the main uncertainty cause. Because of the noise, the circumferences in Fig. 6 become rings whose thickness depends on the noise level and on the sensor working point (Fig. 8). Simulations have been carried out considering a sensor arrangement similar to that described in the experimental result section, which is based on plastic optical fibers having a core diameter of 980 μm, numerical aperture of 0.5, and fiber distance d_0 = 3 mm. The optical power collected by the receiving fibers has been computed for positions of the transmitting fiber in the range of (-5 mm $\div$ 5 mm) x (-5 mm $\div$ 5 mm) and considering a constant noise level whose amplitude is 0.1 % of the maximum detected signal. At each position the corresponding power circumferences have been computed and then converted into rings (or annuli) to take into account the effect of noise, thus obtaining an intersection area as that shown in Fig. 8. For simplification purposes, the position uncertainty both in the x and y directions has been approximated considering a circle having radius δ that includes the intersection area.

Results obtained considering different fiber separations are shown in Fig. 9, which depicts the area where the sensor uncertainty is better than 50 μm; it is possible to see that the best range can be obtained minimizing the fiber separation, as already predicted by Eqn. 3.

The effect of the fiber distance d_0 has been analyzed too and the results are shown in Fig. 10 in which the sensor range corresponding to an uncertainty of 50 μm has been derived for distances 3 mm, 4 mm, 6 mm and 8 mm and for a constant separation d_{F} = 2 mm. The range is proportional to the fiber

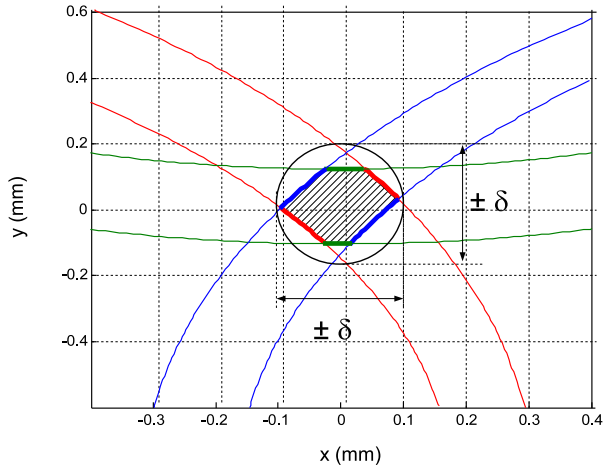

Fig. 8. Circle intersections in presence of noise on the detected signals and estimation of the position uncertainty δ.

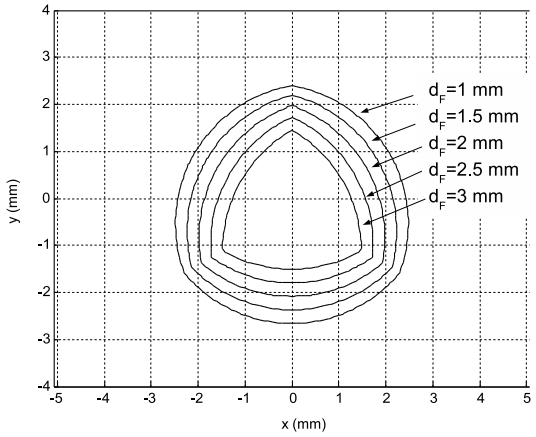

Fig. 9. Sensor working range for different fiber separations d_{F}.

distance since for increasing values the light spots become larger. However, for longer distances the noise presence causes uncertainties exceeding 50 μm in the central part of the range, at positions where the transmitting fiber is completely illuminating one of the receiving fiber, which is a conditions of minimum (ideally null) sensitivity to displacement.

IV. Experimental results

A. Sensor prototype and interrogation system structure

A prototype has been built following the scheme of Fig. 1. Ideally the sensor should be fabricated by embedding the fibers into liquid polymers, so it is possible to obtain a small form factor device with also low loss in the beam deflection using optimized prisms or mirrors. However, to simplify the realization, the fibers have been positioned in grooves made on two rectangular PMMA plates cut to resemble the common mechanical crack monitoring devices and then fixed using epoxy glue. Since standard step-index POF made with a single core exhibit very high loss for small curvature radii, the sensor has been arranged using multicore polymeric fibers, which present negligible attenuation even for a curvature radius smaller than 1 cm.

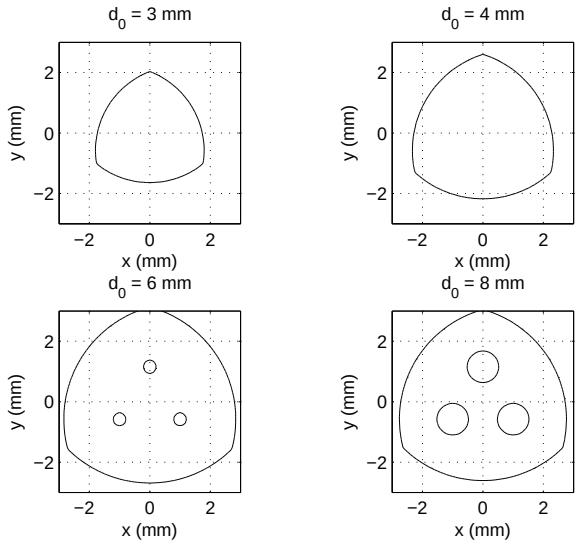

Fig. 10. Working ranges at different fiber distances d_0 and for fiber separation d_{F}= 2 mm.

The use of multicore fibers having 0.6 numerical aperture and 1 mm diameter has been limited to the part of the sensor within the plates. Then, standard 1 mm step-index POF having the same diameter and attenuation of about 0.2 $\mathrm{dB/m}$ have been connected to the multicore fibers using a refractive index matching glue. This solution has the advantage to maintain the cost low since standard single core fibers are less expensive than the multicore, even though the connection between the two type of fibers presents non negligible insertion loss that slightly reduce the sensor performance.

The plate hosting the transmitting fiber has been milled to form a 3 mm deep, $1\,\mathrm{cm}^2$ hole, so that when the transmitting fiber is positioned in the center of the hole, the distance between the transmitting and receiving fiber tips creates a gap d_0 of about 3 mm; this way, according to Eq. 3, it is possible to increase the sensor working range while maintaining an acceptable signal-to-noise ratio. The distance between the fibers axis d_{F} was set to about 2 mm. In order to reduce the effect of stray light and thus prevent crosstalk at the receivers, the sides of the receiving fiber tips have been covered with black paintings. A picture of the prototype is shown in Fig. 11 where the upper plate contains the receiving fibers and the lower the transmitting one. The multicore/single-core joint is also visible in the picture.

A different sensor arrangement was investigated in a previous work [16]: in that case straight fibers were used, avoiding thus the additional bending induced loss so it was possible to work with higher optical signal levels although at the expense of the sensor dimensions that could limit its usage in practical crack monitoring application.

The sensor prototype is connected to a home-made interrogation system using: (i) the red LED source, driven by a modulated current signal at f = 620 Hz to allow a synchronous detection in order to reduce the effect of noise and environmental light disturbances; (ii) three receivers employing a classical scheme based on photodiodes (PD) connected to

transimpedance amplifiers having 1 MΩ gain; (iii) a data acquisition board connected to a PC to analyze the acquired synchronous data with a Noise Equivalent Bandwidth (NEB) of 10 Hz.

Both the LED and the PD are produced by Ratioplast and are mounted in a metal receptacle equipped with a SMA connector suitable for POF. The LED emission peak is at 650 nm, while the optical power measured through a short span of fiber is about 140 μW. The optical power available at the sensor, however, is significantly lower because of the fiber attenuation and losses: for a 10 m span of single core SI-POF a value of about 92 μW has been measured. This value is further reduced if there are sharp fiber bends. For example, the measured optical power becomes 58 μW after a half turn with 3 cm diameter. The sensitivity to bending is a known issue for optical fibers, especially for SI-POF, and it affects the performance of the proposed sensor as well as of any other sensor based on the measurement of the light intensity. If the variation of losses with bends is critical, multicore fibers should be preferred also for the link that connects the interrogation system to the sensor, although this may imply a higher overall attenuation. In order to highlight the benefit provided by multicore fibers, the same optical power measurement has been repeated for a span of 10 m of a multicore fiber obtaining a value of 57.3 μW in absence of sharp bends, and of 57.2 μW with a half turn bending having a diameter of 3 cm.

The optical power distribution has been measured at the surface of the fiber tip through a near-field measurement setup based on a CCD camera. The obtained light intensity distribution for the fiber used in the proposed sensor is shown in Fig. 12, where it is possible to see that the intensity in the central part of the fiber is higher than in the outside region. This distribution does not change significantly even when the fiber is bent as described before.

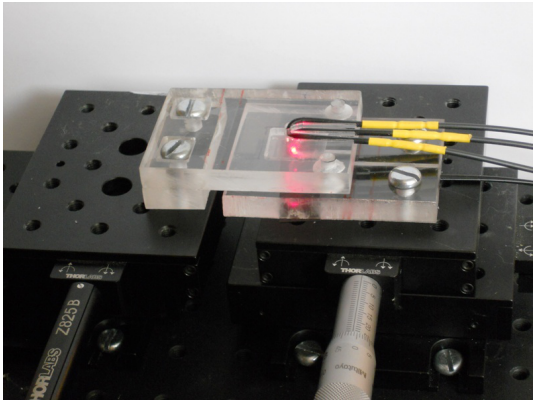

Fig. 11. Setup employed to characterize and test the 2-D fiber sensor prototype.

B. Sensor characterization

The sensor prototype has been characterized with two computer-controlled precision linear translation stages, shown in Fig. 11, having uncertainty lower than 10 μm. The sensor response has been measured by moving the transmitting fiber

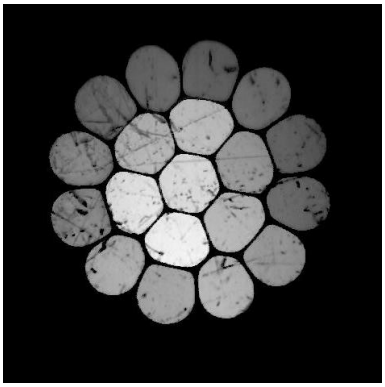

Fig. 12. Measured power distribution employing a multicore fiber.

plate in a region (-5 mm ÷ 5 mm) x (-5 mm ÷ 5 mm), in 0.1 mm steps, while acquiring for each receiver the correspondent output voltage. The three acquired signals are shown in Fig. 13 where it is possible to note that the maximum acquired signal has an amplitude of about 0.25 V and that the peaks have a significative amplitude difference; this is mainly because of the difficulty in obtaining the parallel alignment of the receiving fibers with the home-made fixture.

The sensor response is rather different from the response expected considering only the optical power shown in Fig. 12 and this is because the sensor response depends not only on the light power distribution at the transmitting fiber tip, but also on the averaging effect operated by the receiving fiber that collects the light throughout the surface of its tip.

To implement the calibration procedure, a fitting of the received voltages has been performed considering that the light intensity emitted from the fiber has a Gaussian shape:

$$V_{\text{out}} = A \cdot e^{-\frac{1}{k}\cdot[(x-x_0)^2+(y-y_0)^2]} + V_0 \qquad (4)$$

where x and y represent the coordinates in the plane of the transmitting fiber, V_0 the voltage offset, which is mainly due to the offset of the amplifiers, and the terms x_0, y_0, A, k are related to light intensity distribution as measured by the receiving fibers.

An example of the difference between the fitted gaussian models and the acquired voltages is shown for one of the receiving fibers in Fig. 14, where it is possible to see that the maximum voltage difference is of about 5 mV. Similar results have been obtained for the other two receiving fibers. This is a model error whose effects are not negligible since the signal noise, measured in a position where the detected signal is zero, is of about 0.5 mV.

The performance of the calibration procedure has been evaluated computing the difference between the nominal position, which is fixed using the translation stages, and the position computed from the three amplifier outputs and based on the circle intersection procedure previously described.

As an example, Fig. 15 shows the case where the transmitting fiber is positioned at P = $(50 \pm 10, -650 \pm 10)$ μm. The position has been set and measured through the translation stages. Three circles have been thus derived using the fitted Gaussian models and the acquired voltages. The intersection

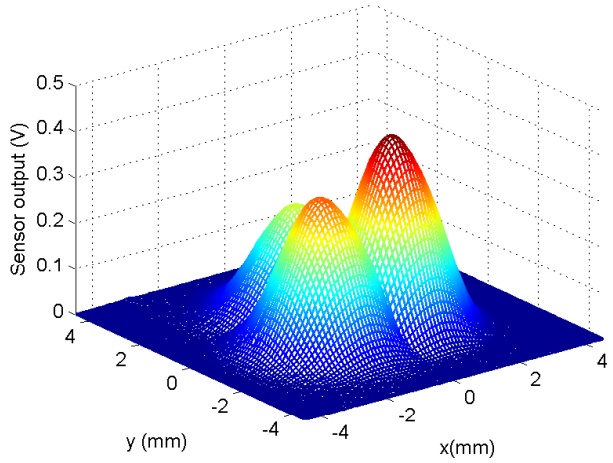

Fig. 13. Experimental readings from the three receivers in the (± 4 x ± 4) mm range.

of the circumferences is detailed in Fig. 16. In this figure the nominal position P is marked by a dot and its uncertainty is represented with a rectangle; then, as already mentioned, the uncertainty in the position determination is given by the area delimited by the intersections among the circumferences. As shown in Fig. 8 this area has been approximated with a circle that, in this example, has a radius δ of approximately 25 μm. This uncertainty takes into account the main contributions such as the effects of the model error (Fig. 14) the signal noise and the short-term stability (some hours) that is mainly due to the fibers and to the interrogation system.

The test procedure has been repeated for several points in the range of ± 4 mm x ± 4 mm thus obtaining the uncertainty distribution shown in Fig. 17. The uncertainty is of about 20 μm in the central part of the figure, that is where the transmitting fiber is faced to the receiving fibers, and below 50 μm inside an approximatively circular area having diameter of about 3 mm.

The sensor range is thus of about ± 1.5 mm when a target uncertainty of 50 μm is considered, a value slightly lower than what expected from simulations due to the model errors not taken into account in the simulations.

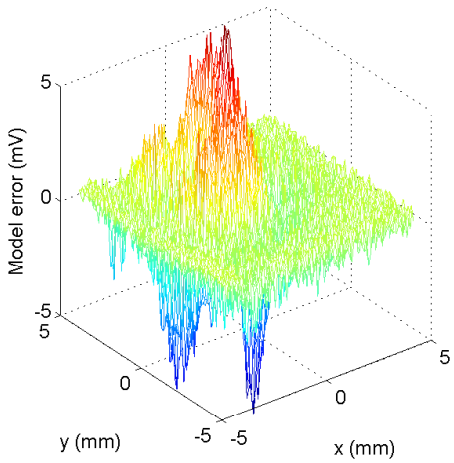

Fig. 14. Example of the difference between the voltage acquired by a receiving fiber and the Gaussian model obtained by a fitting of the acquired data.

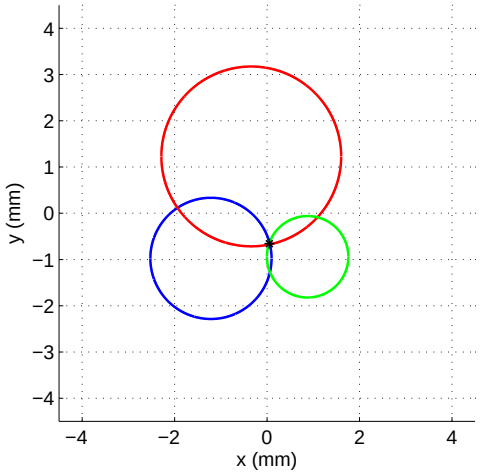

Fig. 15. Three-circles intersection when the transmitter position is in P = $(50 \pm 10, -650 \pm 10)$ μm.

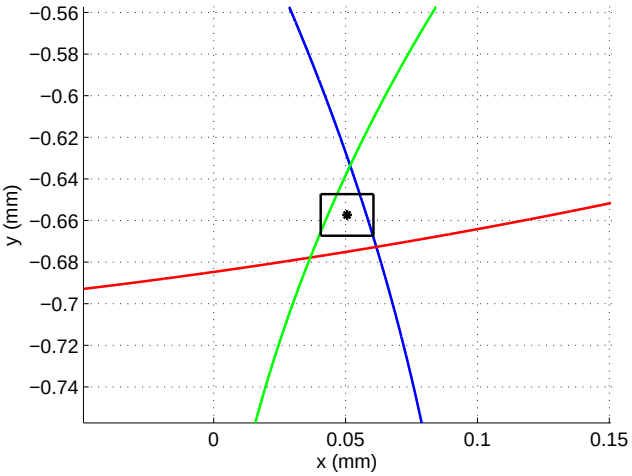

Fig. 16. Detail of the circle intersection and the position measured using the translation stages; the black rectangle represents the stages uncertainty.

V. Conclusion

A low-cost fiber based sensor for 2D displacement measurements has been presented and its performance evaluated. The sensor is made by plastic optical fibers embedded into two plates that can slide relative to each other. The displacement is calculated from the variation in the power transmitted through facing fibers that become misaligned because of the displacement.

Experimental tests have been carried out using two plates embedding one transmitting fiber and three receiving fibers having 1 mm diameter. The results obtained when the gap

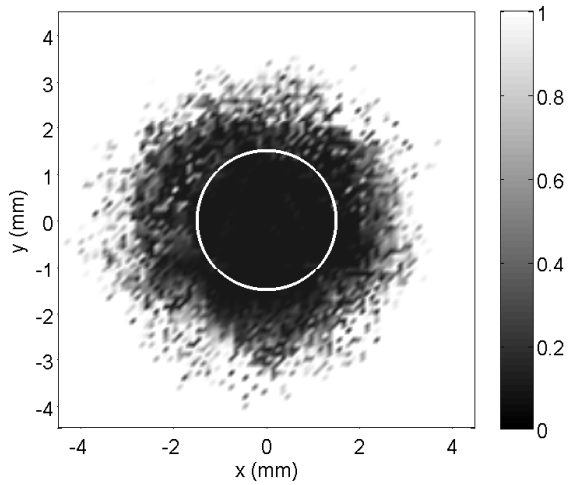

Fig. 17. Map of the uncertainty distribution; the white circle encloses the area for which the uncertainty is below $50\,\mu$m.

between the plates is of about 3 mm have shown that the sensor working range is of about $\pm$1.5 mm x $\pm$1.5 mm and the position can be obtained with an uncertainty better than $\pm 50\ \mu$m in both directions, thus confirming that the proposed approach is a viable solution to traditional mechanical systems.

REFERENCES

[1] F. Ansari, "Sensing issues in civil structural health monitoring", *Springer*, 2005.

[2] J.H. Williams, A. Davies, P.R. Drake, "Condition-based maintenance and machine diagnostics", *Springer*, 1994.

[3] $http://www.prginc.com/Masonry/PRG-crackmon.html$

[4] R. Djugum, "Strain gauges", *VDM Verlag*, 2009.

[5] B. Glisic, D. Inaudi, "Fibre optic methods for structural health monitoring", *JohnWiley and Sons Ltd.*, 2007.

[6] G. Zhou, L. M. Sim, "Damage detection and assessment in fibre-reinforced composite structures with embedded fibre optic sensors-review", *Smart Mater. Struct.* 11, pp. 925-939, 2002.

[7] J.M. Lopez-Higuera, L. Rodriguez Cobo, A. Quintela Incera,"Fiber optic sensors in structural health monitoring", *J. Lightwave Technol.*, 29, pp. 587-608, 2011.

[8] T.W. Graver, D. Inaudi, J. Doornink, "Growing market acceptance for fiber-optic solutions in civil structures", 2004, available online: *http://www.micronoptics.com*

[9] S. Corbellini, M. Parvis, S. Grassini, L. Benussi, S. Bianco, S. Colafranceschi, D. Piccolo "Modified POF sensor for gaseous hydrogen fluoride monitoring in the presence of ionizing radiations", *IEEE Trans. Instrum. Meas.*, 61(5), pp. 1201-1208, 2012

[10] K. Peters, "Polymer optical fiber sensors: a review", *Smart Mater Struct*, 20, 2011, pp. 1-17.

[11] A. Vallan, M.L. Casalicchio, G. Perrone, "Displacement and acceleration measurements in vibration tests using a fiber optic sensor", *IEEE Trans. Instr. Meas.*, 59(5), pp. 1389-1396, 2010.

[12] G. Perrone, A. Vallan, "A low-cost optical sensor for non contact vibration measurements", *IEEE Trans. Instrum. Meas.*, 58(7), pp. 1650-1656, 2009

[13] J.B. Faria, "A Theoretical Analysis of the Bifurcated Fibre Bundle Displacement Sensor", *IEEE Trans. Instrum. Meas.*, 47(3), pp. 742-747, 1998.

[14] J. Mateo, M. A. Losada, I. Garcés, J. Zubia, "Global characterization of optical power propagation in step-index plastic optical fibers", *OPTICS EXPRESS*, 14(20), pp. 9028-9035.

[15] *http://slwti.com/FA-2D.aspx*

[16] M.L. Casalicchio, M. Olivero, A. Penna, G. Perrone, A. Vallan, "Low-cost 2D fiber-based displacement sensor", *Proc. of IEEE International Instrumentation and Measurement Technology Conference (I2MTC 2012)*, Graz, Austria, May 13-16, pp. 2078-2082, 2012

PLACE PHOTO HERE

Alberto Vallan received the M.S. degree in Electronic Engineering from Politecnico di Torino (Italy) in 1996 and the Ph.D. degree in Electronic Instrumentation from the University of Brescia (Italy) in 2000. He is currently assistant professor of Electronic Measurements at Politecnico di Torino, Department of Electronics and Telecommunications. His main research interests are digital signal processing and development and characterization of sensors and measuring instruments for industrial applications. Dr. Vallan is member of IEEE/I2MTC Society.

PLACE PHOTO HERE

Maria Luisa Casalicchio received the M.S. degree in Electronic Engineering and the Ph.D. degree in Metrology: Measurement Science and Technique from Politecnico di Torino (Italy) in 2007 and in 2012, respectively, and she is currently research assistant at the Department of Electronics and Telecommunications of the same university. Her main fields of interest are the development and the metrological characterization of acquisition systems and fiber optic sensors.

PLACE PHOTO HERE

Massimo Olivero received the M.S. degree in Electronic Engineering and the Ph.D. in Photonics from Politecnico di Torino (Italy) in 2002 and 2006, respectively. In 2004-2005 he worked as a Visiting Researcher at the Technical University of Denmark on the development of integrated optical devices by direct UV writing. From 2006 to 2008 he was post-doctoral researcher at Politecnico di Torino, conducting research on optical measurements and characterization of nanostructured materials. He is currently Senior Technician at the Photonics Lab of Politecnico di Torino, where he works on fiber components for high power lasers and fiber optics sensors.

PLACE PHOTO HERE

Guido Perrone holds a M.S. degree in Electronics Engineering and Ph.D. degree in Electromagnetics from Politecnico di Torino (Italy), where he is currently with the Department of Electronics and Telecommunications as professor of Microwave Components and of Optical Fibers and Components. His research activity is mainly in the fields of fiber optic sensors and of high power fiber lasers. Dr. Perrone is member of IEEE/MTTS, of IEEE/Photonics Society and of the Optical Society of America.